#### PHYSICAL REVIEW D **89**, 051102(R) (2014)

### Evidence for $\nu_{\mu} \rightarrow \nu_{\tau}$ appearance in the CNGS neutrino beam with the OPERA experiment

N. Agafonova, <sup>1</sup> A. Aleksandrov, <sup>2</sup> A. Anokhina, <sup>3</sup> S. Aoki, <sup>4</sup> A. Ariga, <sup>5</sup> T. Ariga, <sup>5</sup> T. Asada, <sup>6</sup> D. Autiero, <sup>7</sup> A. Ben Dhahbi, <sup>5</sup> A. Badertscher, <sup>8</sup> D. Bender, <sup>9</sup> A. Bertolin, <sup>10</sup> C. Bozza, <sup>11</sup> R. Brugnera, <sup>12,10</sup> F. Brunet, <sup>13</sup> G. Brunetti, <sup>5</sup> A. Buonaura, <sup>2,14</sup> S. Buontempo, <sup>2</sup> B. Büttner, <sup>15</sup> L. Chaussard, <sup>7</sup> M. Chernyavsky, <sup>16</sup> V. Chiarella, <sup>17</sup> A. Chukanov, <sup>18</sup> L. Consiglio, <sup>2</sup> N. D'Ambroio, <sup>19</sup> G. De Lellis, <sup>2,14</sup> M. De Serio, <sup>20,21</sup> P. Del Amo Sanchez, <sup>13</sup> A. Di Crescenzo, <sup>2,\*</sup> D. Di Ferdinando, <sup>22</sup> N. Di Marco, <sup>19</sup> S. Dmitrievski, <sup>18</sup> M. Dracos, <sup>23</sup> D. Duchesneau, <sup>13</sup> S. Dusini, <sup>10</sup> T. Dzhatdoev, <sup>3</sup> J. Ebert, <sup>15</sup> A. Ereditato, <sup>5</sup> J. Favier, <sup>13</sup> T. Ferber, <sup>15,†</sup> G. Ferone, <sup>2,14</sup> R. A. Fini, <sup>20</sup> T. Fukuda, <sup>24</sup> G. Galati, <sup>20,21</sup> A. Garfagnini, <sup>12,10</sup> G. Giacomelli, <sup>25,22</sup> C. Goellnitz, <sup>15</sup> J. Goldberg, <sup>26</sup> Y. Gormushkin, <sup>18</sup> G. Grella, <sup>11</sup> F. Grianti, <sup>17</sup> M. Guler, <sup>9</sup> C. Gustavino, <sup>27</sup> C. Hagner, <sup>15</sup> K. Hakamata, <sup>6</sup> T. Hara, <sup>4</sup> T. Hayakawa, <sup>6</sup> M. Hierholzer, <sup>15,5</sup> A. Hollnagel, <sup>15</sup> B. Hosseini, <sup>2,14</sup> H. Ishida, <sup>24</sup> K. Ishiguro, <sup>6</sup> M. Ishikawa, <sup>6</sup> K. Jakovcic, <sup>28</sup> C. Jollet, <sup>23</sup> C. Kamiscioglu, <sup>29</sup> M. Kamiscioglu, <sup>9</sup> T. Katsuragawa, <sup>6</sup> J. Kawada, <sup>5</sup> H. Kim, <sup>30</sup> S. H. Kim, <sup>30,8</sup> M. Kimura, <sup>5</sup> N. Kitagawa, <sup>6</sup> B. Klicek, <sup>28</sup> K. Kodama, <sup>31</sup> M. Komatsu, <sup>6</sup> U. Kose, <sup>10</sup> I. Kreslo, <sup>5</sup> A. Lauria, <sup>2,14</sup> J. Lenkeit, <sup>15</sup> A. Ljubicic, <sup>28</sup> A. Longhin, <sup>17,1</sup> P. Loverre, <sup>32,27</sup> A. Malgin, <sup>1</sup> G. Mandrioli, <sup>21</sup> J. Marteau, <sup>7</sup> T. Matsuo, <sup>24</sup> V. Matveev, <sup>1</sup> N. Mauri, <sup>25,22</sup> E. Medinaceli, <sup>12,10</sup> A. Meregaglia, <sup>23</sup> P. Migliozzi, <sup>2</sup> S. Mikado, <sup>24</sup> M. Miyanishi, <sup>6</sup> E. Miyashita, <sup>6</sup> P. Monacelli, <sup>33</sup> M. C. Montesi, <sup>21,4</sup> K. Morishima, <sup>6</sup> M. T. Muciaccia, <sup>20,21</sup> N. Naganawa, <sup>6</sup> T. Naka, <sup>6</sup> N. Nakamura, <sup>6</sup> T. Nakano, <sup>6</sup> Y. Nakatsuka, <sup>6</sup> K. Niwa, <sup>6</sup> S. Ogawa, <sup>24</sup> N. Okateva, <sup>16</sup> A. Olshevsky, <sup>18</sup> T. Omura, <sup>6</sup> K. Ozaki, <sup>8</sup> A. Paoloni, <sup>17</sup> B. D. Park, <sup>30</sup> A. Pastore, <sup>20</sup> C. Patrizili, <sup>9</sup> R. Rescigno, <sup>11</sup> M. Roda, <sup>1</sup>

#### (OPERA Collaboration)

<sup>1</sup>INR Institute for Nuclear Research, Russian Academy of Sciences RUS-117312 Moscow, Russia <sup>2</sup>INFN Sezione di Napoli, I-80125 Napoli, Italy <sup>3</sup>SINP MSU-Skobeltsyn Institute of Nuclear Physics, Lomonosov Moscow State University, RUS-119992 Moscow, Russia <sup>4</sup>Kobe University, J-657-8501 Kobe, Japan <sup>5</sup>Albert Einstein Center for Fundamental Physics, Laboratory for High Energy Physics (LHEP), University of Bern, CH-3012 Bern, Switzerland <sup>6</sup>Nagoya University, J-464-8602 Nagoya, Japan <sup>7</sup>IPNL, Université Claude Bernard Lyon 1, CNRS/IN2P3, F-69622 Villeurbanne, France Institute for Particle Physics, ETH Zurich, CH-8093 Zurich, Switzerland <sup>9</sup>METU Middle East Technical University, TR-06531 Ankara, Turkey <sup>10</sup>INFN Sezione di Padova, I-35131 Padova, Italy <sup>11</sup>Dipartimento di Fisica dell'Uni. di Salerno and "Gruppo Collegato" INFN, I-84084 Fisciano (SA), Italy <sup>12</sup>Dipartimento di Fisica dell'Università di Padova, I-35131 Padova, Italy <sup>13</sup>LAPP, Université de Savoie, CNRS IN2P3, F-74941 Annecy-le-Vieux, France <sup>14</sup>Dipartimento di Scienze Fisiche dell'Università Federico II di Napoli, I-80125 Napoli, Italy <sup>15</sup>Hamburg University, D-22761 Hamburg, Germany <sup>16</sup>LPI-Lebedev Physical Institute of the Russian Academy of Sciences, 119991 Moscow, Russia <sup>17</sup>INFN-Laboratori Nazionali di Frascati dell'INFN, I-00044 Frascati (Roma), Italy <sup>18</sup>JINR-Joint Institute for Nuclear Research, RUS-141980 Dubna, Russia <sup>19</sup>INFN-Laboratori Nazionali del Gran Sasso, I-67010 Assergi (L'Aquila), Italy <sup>20</sup>INFN Sezione di Bari, I-70126 Bari, Italy <sup>21</sup>Dipartimento di Fisica dell'Università di Bari, I-70126 Bari, Italy <sup>22</sup>INFN Sezione di Bologna, I-40127 Bologna, Italy <sup>23</sup>IPHC, Université de Strasbourg, CNRS/IN2P3, F-67037 Strasbourg, France <sup>24</sup>Toho University, J-274-8510 Funabashi, Japan <sup>25</sup>Dipartimento di Fisica dell'Università di Bologna, I-40127 Bologna, Italy <sup>26</sup>Department of Physics, Technion, IL-32000 Haifa, Israel <sup>27</sup>INFN Sezione di Roma, I-00185 Roma, Italy <sup>28</sup>IRB-Rudjer Boskovic Institute, HR-10002 Zagreb, Croatia

<sup>29</sup>Ankara University, TR-06100 Ankara, Turkey
 <sup>30</sup>Gyeongsang National University, ROK-900 Gazwa-dong, Jinju 660-701, Korea
 <sup>31</sup>Aichi University of Education, J-448-8542 Kariya (Aichi-Ken), Japan
 <sup>32</sup>Dipartimento di Fisica dell'Università di Roma 'La Sapienza' and INFN, I-00185 Roma, Italy
 <sup>33</sup>Dipartimento di Fisica dell'Università dell'Aquila and INFN, I-67100L'Aquila, Italy
 <sup>34</sup>ITEP-Institute for Theoretical and Experimental Physics, RUS-317259 Moscow, Russia
 <sup>35</sup>Utsunomiya University, J-321-8505 Tochigi-Ken, Utsunomiya, Japan
 <sup>36</sup>Dipartimento di Fisica dell'Università di Milano-Bicocca, I-20126 Milano, Italy
 <sup>37</sup>IIHE, Université Libre de Bruxelles, B-1050 Brussels, Belgium
 (Received 5 November 2013; published 5 March 2014)

The OPERA experiment is designed to search for  $\nu_{\mu} \to \nu_{\tau}$  oscillations in appearance mode, i.e., through the direct observation of the  $\tau$  lepton in  $\nu_{\tau}$ -charged current interactions. The experiment has taken data for five years, since 2008, with the CERN Neutrino to Gran Sasso beam. Previously, two  $\nu_{\tau}$  candidates with a  $\tau$  decaying into hadrons were observed in a subsample of data of the 2008–2011 runs. Here we report the observation of a third  $\nu_{\tau}$  candidate in the  $\tau^- \to \mu^-$  decay channel coming from the analysis of a subsample of the 2012 run. Taking into account the estimated background, the absence of  $\nu_{\mu} \to \nu_{\tau}$  oscillations is excluded at the 3.4  $\sigma$  level.

DOI: 10.1103/PhysRevD.89.051102 PACS numbers: 14.60.Pq, 14.60.Lm

#### I. INTRODUCTION

The OPERA experiment is designed to perform a crucial test of neutrino oscillations aiming at the direct observation of the appearance of  $\tau$  neutrinos in a  $\nu_{\mu}$  beam. Using atmospheric neutrinos, the Super-Kamiokande experiment recently reported the evidence for a  $\nu_{\tau}$  appearance signal on a statistical basis and with a low signal-to-noise ratio [1]. The OPERA apparatus has the capability of detecting the  $\nu_{\tau}$ -charged current interactions on an event-by-event basis and with an extremely high signal-to-noise ratio. A positive evidence from OPERA can prove that the  $\nu_{\mu} \rightarrow \nu_{\tau}$  transition is the mechanism underlying the disappearance of muon neutrinos at the atmospheric scale [2], thus providing essential support to the establishment of the three-flavor mixing scheme.

To accomplish this task, several ingredients are required: a high-energy neutrino beam, a long baseline and a kt-scale detector with submicrometric resolution. The CERN Neutrinos to Gran Sasso (CNGS [3]) beam was designed to deliver muon neutrinos with a mean energy of 17 GeV to the Gran Sasso underground laboratory (LNGS) where the detector is installed at a distance of 730 km. The contaminations of  $\bar{\nu}_{\mu}$ - and  $\nu_e + \bar{\nu}_e$ -charged current interactions at LNGS, relative to the number of  $\nu_{\mu}$ -charged current

interactions, are 2.1% and 0.9%, respectively. The contamination from prompt  $\nu_{\tau}$  is negligible.

The OPERA detector [4] is composed of two identical supermodules, each consisting of an iron spectrometer downstream of a target section. The target has a mass of about 1.2 kt and a modular structure with approximately 150,000 target units, called bricks. A brick is made of 56 1-mm-thick lead plates, acting as targets, interleaved with 57 nuclear emulsion films, used as micrometric tracking devices. Each film is composed of two 44-µm-thick emulsion layers on both sides of a 205-μm-thick plastic base. Bricks are arranged in walls interleaved with planes of scintillator strips forming the target tracker (TT). The magnetic spectrometers, which consist of iron magnets instrumented with resistive plate chambers (RPC) and precision drift tubes (PT), are used for the measurement of the muon charge and momentum. For each event, the information provided by the electronic detectors allows assigning to each brick a probability to contain the neutrino interaction vertex.

In a recent publication [5] the  $\nu_{\tau}$  appearance analysis was described in detail, explaining the selection of signal candidate events and the assessment of efficiencies and backgrounds. In the following, the experimental procedure is briefly summarized along with the description of a third  $\nu_{\tau}$  candidate.

## dicrescenzo@na.infn.it \*\*Present address: Doutsehes Flektronen Synchrotren (DESV) II DATA

\*Corresponding author.

#### II. DATA SAMPLE

The CNGS beam has run for five years, from 2008 till the end of 2012, delivering a total of  $17.97 \times 10^{19}$  protons on target (pot) yielding 19,505 neutrino interactions recorded in the targets.

A neutrino interaction is classified as being either charged currentlike  $(1 \mu)$  or neutral currentlike  $(0 \mu)$  by using the electronic data of the TT and the spectrometers.

<sup>&</sup>lt;sup>T</sup>Present address: Deutsches Elektronen Synchrotron (DESY), 22607 Hamburg, Germany.

<sup>&</sup>lt;sup>‡</sup>Present address: LHEP, University of Bern, CH-3012 Bern, Switzerland.

<sup>§</sup>Present address: Kyungpook National University, Daegu, Korea.

<sup>&</sup>quot;Corresponding author. longhin@lnf.infn.it

Present address: Samsung Changwon Hospital, SKKU, Changwon, Korea.

#### EVIDENCE FOR $\nu_{\mu} \rightarrow \nu_{\tau}$ APPEARANCE ...

The neutrino interaction vertex brick predicted by the electronic detector data is extracted from the target by an automatic brick manipulator system. If the scanning of a dedicated pair of emulsion films [changeable sheets (CS)], acting as an interface between the brick and the TT, yields tracks related to the neutrino interaction, the emulsion films of the brick are developed and distributed to the different scanning laboratories of the collaboration. Their analysis provides the three-dimensional reconstruction of the neutrino interaction and of possible secondary decay vertices of short-lived particles with micrometric accuracy.

The sample of events considered in our previous publication [5] consisted of

- (a) all of the 0  $\mu$  events collected and searched for in the two most probable bricks for the 2008–2009 runs and in the most probable one for the 2010–2011 runs.
- (b) all of the 1  $\mu$  events with  $p_{\mu} < 15 \text{ GeV}/c$  collected and searched for in the two most probable bricks for the 2008–2009 runs and in the most probable one for the 2010 run.

Two  $\nu_{\tau}$  candidate events in the hadronic decay channels were observed: the first in the 2009 run data with a one-prong topology [6] and the second in the 2011 run data with a three-prong topology [5].

The results reported in this paper are based on the extension of the analysis to the most probable bricks of 1  $\mu$  events with  $p_{\mu} < 15~{\rm GeV}/c$  collected during the 2011 and 2012 runs. This corresponds to an increase of the analyzed pot of 12%. A  $\nu_{\tau}$  candidate event in the muonic decay channel was observed in this data sample.

#### III. THE NEW $\nu_{\tau}$ CANDIDATE EVENT

Figure 1 shows the electronic detector display of this new event; the neutrino vertex brick (highlighted) is well contained in the target region. An isolated, penetrating track is reconstructed in the electronic detectors: the particle is recorded in 24 planes of the TT and crosses six RPC planes before stopping in the spectrometer. This range corresponds to 1650 g/cm<sup>2</sup> of material.

Four RPC planes have hits associated to the track in both projections (Fig. 1). The time spread of the RPC hits is within 20 ns. The efficiency of the RPC planes was monitored with cosmic ray tracks and muons from neutrino interactions in the rock [7].

The muon momentum at the interaction vertex is accurately estimated from the range of the particle in the electronic detector: a Kalman filter-based algorithm yields a value of  $p_{\mu}=(2.8\pm0.2)~{\rm GeV}/c$ . The momentum estimate resulting from a measurement of multiple Coulomb scattering (MCS) [8] in the downstream brick, based on the emulsion data, leads to a compatible value of  $3.1_{-0.5}^{+0.9}~{\rm GeV}/c$ .

For events to be retained as candidates in the  $\tau \to \mu$  decay channel, the charge of the secondary muon track must either be measured to be negative or be undetermined.

#### PHYSICAL REVIEW D 89, 051102(R) (2014)

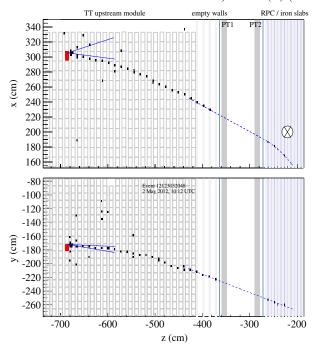


FIG. 1 (color online). Electronic detector display of the new  $\nu_{\tau}$  candidate event. The blue solid lines represent the linear extrapolation of tracks measured in the emulsion films of the vertex brick. The dashed blue lines show the fit of the most downstream hits according to the model:  $x(z) = p_{0x} + p_{1x}(z-z_0) + p_{2x}(z-z_0)^2$  with  $z_0 = -267.826$  cm. The quadratic term parameter is  $p_{2x} = (-0.00389 \pm 0.00069)$  cm<sup>-1</sup>, and the fit  $\chi^2/ndf$  is 2.6/4.

This requirement is applied in order to minimize the background from charged current  $\nu_{\mu}$  interactions with production of a charmed particle decaying to a positive muon and where the primary negative muon goes undetected.

The charge measurement is performed using the bending of the track in the magnetized iron given by the four available RPC hits.

For this event, no hits could be recorded by the PT planes (grey rectangles in Fig. 1) due to an inefficiency of the trigger (the trigger is given by a two out of three majority of the first RPC plane within the magnet and two upstream dedicated RPC planes, the so-called XPC planes [4]).

As the last brick-filled wall is followed by three double layers of TT planes (and essentially no other material, see Fig. 1), the slope of the track at the entrance of the spectrometer could be determined with the needed precision.

The relative alignment of RPC and TT planes in the *x* and *y* directions was determined using muons from interactions of neutrinos in the rock (horizontal tracks) and cosmic ray muons (sensitive also to vertical displacements). In both cases, the resulting alignment is accurate at the millimeter level. The errors on the measurement points were computed assuming uniform probability density

across the strips that have a width of 2.6 cm(x) and 3.5 cm(y) for RPC detectors and 2.64 cm for the TT. The uncertainty related to MCS has also been taken into account.

The TT and RPC hits are fitted with a simple analytical model consisting of a straight line in the field-free region matched to a parabola in the magnetized region (Fig. 1). The fitted parabola bends towards smaller x (see Fig. 1 top) corresponding to a negative charge. The quadratic parameter is nonzero at 5.6  $\sigma$  significance. The associated momentum at the spectrometer entrance is compatible with the one measured from range.

For this event, the charge misidentification probability was estimated by means of a Monte Carlo simulation. Muons of either charge were sampled using a uniform momentum distribution. A Gaussian smearing of the incoming direction was applied to account for the measurement error in the three most downstream TT layers. Only those muons stopping in the same slab observed for the event and with hits within a time window of 30 ns were selected, giving a sample of negative (positive) muons with an average momentum of 613 MeV/c with a 48 MeV/c rms (540 MeV/c with a 26 MeV/c rms). The strip readout was simulated using the efficiency observed in real data. The resulting distributions of the quadratic term  $p_{2x}$  for the  $\mu^-$  and  $\mu^+$  samples are shown in Fig. 2. The fraction of  $\mu^+$ for which the bending is reconstructed as negative and that mimics a  $\mu^-$  is 2.5%, but for only 0.063% of the  $\mu^+$  is the bending more negative than the observed one. The measured  $p_{2x}$  is compatible with the peak value of the distribution for the  $\mu^-$  sample. For this event, the sign of the charge of the secondary muon is thus univocally determined to be negative. The efficiency of the RPC chamber downstream of the iron slab layer in which the muon is assumed to have stopped is 93%. If the muon had actually stopped in the next layer with this RPC plane being inefficient, then its momentum would have been larger by only 75 MeV/c, the precision in its charge determination

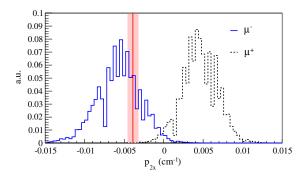


FIG. 2 (color online). Distributions of  $p_{2x}$  for a Monte Carlo sample of  $\mu^-$  and  $\mu^+$ . The vertical solid line represents the measured value, and the vertical band corresponds to the  $1\sigma$  confidence interval. The visible structures are due to the pitch of the RPC readout which introduces a discretization effect.

remaining unaffected. The reliability of the simulation has been cross-checked with data [7,9].

#### IV. EVENT TOPOLOGY AND KINEMATICS

The scanning of the CS films of the interaction brick yielded a track matching the muon direction. A converging pattern of more tracks was also found, reinforcing the conditions for event validation.

The neutrino interaction occurred well inside the brick with respect to the longitudinal direction, 3.3  $X_0$  from its downstream face. All tracks possibly related to the interaction were searched for in the brick with an angular acceptance up to  $\tan \theta = 1$ . The display of the event as reconstructed in the brick is shown in Fig. 3.

The primary vertex  $(V_0)$  is given by two tracks: the  $\tau$  lepton candidate and a hadron track  $(p_0)$  having a distance of closest approach of  $(0.5 \pm 0.5)~\mu m$ . An electromagnetic shower produced by a  $\gamma$  ray and pointing to this primary vertex has also been observed. The  $\tau$  lepton decay occurs in the plastic base of the film immediately downstream of the primary vertex, after a flight length of  $(376 \pm 10)~\mu m$ . The longitudinal coordinate of the decay vertex  $(V_1)$  with respect to the downstream face of the lead plate containing the primary vertex  $(z_{\rm dec})$  is  $(151 \pm 10)~\mu m$ .

The kinematical quantities of the tracks measured in the emulsion films are given in the following:

(a) Track  $p_0$  has a momentum  $p_{p_0} = (0.90^{+0.18}_{-0.13}) \text{ GeV/}c$ , measured by MCS. It was found in the CS films. It was followed into the downstream brick where it disappears after having crossed 18 lead plates. No charged particle track could be detected at the interaction point. It is classified as a hadron by its momentum-range correlation [5].

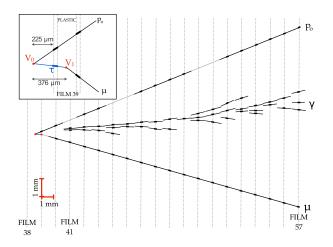


FIG. 3 (color online). Display of the new  $\nu_{\tau}$  candidate event in the xz projection: tracks  $\tau$  and  $p_0$  come from the primary vertex; the  $\tau$  candidate decays in the plastic base of film 39, and track  $d_1$  is the  $\tau$  decay daughter identified as a muon. The starting point of the shower generated from the  $\gamma$  is visible in film 41. The inset contains a zoomed view of the primary and decay vertex region.

EVIDENCE FOR  $\nu_{\mu} \rightarrow \nu_{\tau}$  APPEARANCE ...

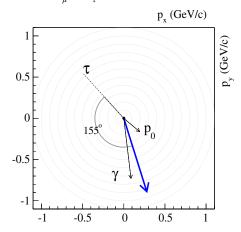


FIG. 4 (color online). The  $\tau$  lepton direction (dashed line) and the momenta of the other primary particles ( $p_0$  and  $\gamma$  ray) in the plane transverse to the CNGS beam. The blue arrow is the sum of the transverse momenta of the  $p_0$  track and of the  $\gamma$  ray.

- (b) Track  $d_1$  is the  $\tau$  decay daughter. Its angle with the  $\tau$  lepton track  $(\theta_{\rm kink})$  is  $(245\pm5)$  mrad. The impact parameter with respect to the primary vertex is  $(93.7\pm1.1)~\mu{\rm m}$ . The track, found also on the CS films, agrees with the muon track reconstructed in the electronic detectors in both momentum  $(\Delta p = 0.3^{+0.9}_{-0.5}~{\rm GeV}/c)$  and angle  $(\Delta \theta = 18\pm25~{\rm mrad})$ .
- (c) The shower originating from a  $\gamma$ -ray conversion has an energy of  $(3.1^{+0.9}_{-0.6})$  GeV. The conversion to an  $e^+e^-$  pair is observed 2.1 mm  $(0.36~X_0)$  downstream of the primary vertex to which it points with an impact parameter of  $(18\pm13)~\mu\text{m}$ . It is incompatible with originating from the secondary vertex, the impact parameter being  $(96\pm12)~\mu\text{m}$ .

A scanning procedure [10] with an extended angular acceptance (up to  $\tan \theta = 3.5$ ) did not reveal any additional large-angle primary track that could be left by a muon or an electron.

In a dedicated search in the 19 films downstream of the primary vertex and in the 10 most upstream films of the downstream brick (more than five  $X_0$  in total), no further  $\gamma$ -ray shower within a slope acceptance of  $\tan \theta < 1$  and an energy above 500 MeV could be found. The single  $\gamma$  ray detected at the primary vertex can be interpreted as coming from the decay of a  $\pi^0$  with the other  $\gamma$  being undetected.

TABLE I. Selection criteria for  $\nu_{\tau}$  candidate events in the  $\tau \to \mu$  decay channel along with the values measured for the candidate event. Variables are defined in the text.

Variable	Selection $(\tau \to \mu)$	Measurement
$\theta_{\rm kink}$ (mrad)	> 20	$245 \pm 5$
$z_{\rm dec} \ (\mu {\rm m})$	< 2600	$151 \pm 10$
$p_{\mu}$ (GeV/c)	[1,15]	$2.8 \pm 0.2$
$p_T^{2ry}$ (MeV/c)	> 250	$690 \pm 50$

PHYSICAL REVIEW D 89, 051102(R) (2014)

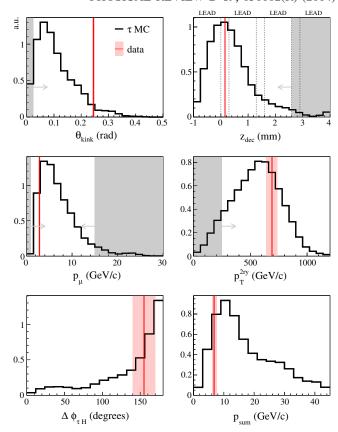


FIG. 5 (color online). Monte Carlo distribution of the reconstructed kinematical variables (see the text) for the  $\tau \to \mu$  decay channel. Red lines show the measured values and red bands their uncertainty. Grey areas cover the regions excluded by the selection cuts.

In the plane transverse to the beam direction, the angle between the  $\tau$  candidate direction and the sum of the transverse momenta of the other primary particles  $(p_0 \text{ and } \gamma)$  is  $\Delta \phi_{\tau H} = (155 \pm 15)^\circ$  (see Fig. 4). The transverse momentum at the secondary vertex  $(p_T^{2ry})$  amounts to  $(690 \pm 50)$  MeV/c. The scalar sum of the momenta of all the particles is  $p_{\text{sum}} = (6.8^{+0.9}_{-0.6})$  GeV/c.

In Table I, the values of the kinematical variables for this event are reported along with the predefined selection criteria [5] for the  $\tau \to \mu$  channel. Besides satisfying all the selections, the variables are well within the domain of the expected signal (see Fig. 5).

# V. EXPECTATIONS AND STATISTICAL SIGNIFICANCE

The method used for the estimation of signal and background was recently discussed [5]. With respect to those results, here we also take into account the extension of the analyzed sample to the  $1\mu$  events of the 2011 and 2012 runs with  $p_{\mu} < 15~{\rm GeV}/c$  (presently completed at 56%).

TABLE II. Signal candidates and background expectations by channel.

Decay channel	Signal candidates	Background events
$\tau \to h$	1	$0.027 \pm 0.005$
$\tau \rightarrow 3h$	1	$0.12 \pm 0.02$
$\tau \to \mu$	1	$0.021 \pm 0.010$
$\tau \rightarrow e$	0	$0.020 \pm 0.004$
Overall	3	$0.184 \pm 0.031$

The total sample of analyzed events is 5272 giving an expected  $\nu_{\tau}$  signal in all decay channels of 1.7 events  $(\Delta m_{23}^2 = 2.32 \times 10^{-3} \text{ eV}^2 \text{ and } \sin^2 2\theta_{23} = 1)$ , out of which 0.54 are in the  $\tau \to \mu$  decay channel.

For the background evaluation, the full sample of 1  $\mu$  events was conservatively accounted for. The total expected background amounts to  $0.184 \pm 0.031$  events. The breakdown in the different channels is reported in Table II, as are the signal candidates. The systematic uncertainties on the signal and on the background are 20% and 17%, respectively.

The background in the  $\tau \to \mu$  channel is dominated by the contribution of large-angle muon scattering in lead (about 80%) followed by charmed particle decays (20%), the background from hadronic interactions with a fake-muon being negligible.

Accounting for the fact that the signal-to-background ratio is different for each decay channel, the following method was adopted: four Poissonian random integers are extracted, one for each decay channel in the background-only hypothesis. The p values of the single channels (obtained as the integral of the Poisson distribution for values larger or equal to the observed number of candidates) are combined into an estimator  $p^* = p_\mu p_e p_h p_{3h}$ . By counting the fraction of extractions for which  $p^* \leq p^*$  (observed), the procedure allows excluding the absence of a  $\nu_\mu \rightarrow \nu_\tau$  oscillation signal with a significance of  $3.4\sigma$  (p value p v

Finally, it should be noted that the new candidate is in a region of the parameter space that is free from background: the  $\tau$  decay occurs in a low-density and low-Z material (the

plastic base) and with a transverse momentum at the secondary vertex of 690 MeV/c, thus highly disfavoring the hypothesis of a large-angle muon scattering.

#### VI. CONCLUSIONS

The results of a  $\nu_{\tau}$  appearance analysis on an extended subsample of the neutrino interactions collected by the OPERA experiment in the CNGS run years 2008 to 2012 are reported. A  $\nu_{\tau}$  candidate event in the  $\tau^- \to \mu^-$  decay channel was observed. A measurement of the negative charge of the  $\tau$  lepton candidate, consistent with what is expected for the  $\nu_{\mu} \to \nu_{\tau}$  oscillation, has been performed for the first time. With the present statistics and the observation of three  $\nu_{\tau}$  candidates, the absence of a signal from  $\nu_{\mu} \to \nu_{\tau}$  oscillations is excluded at 3.4  $\sigma$ .

#### ACKNOWLEDGMENTS

We thank CERN for the successful operation of the CNGS facility and INFN for the continuous support given to the experiment through its LNGS laboratory. We acknowledge funding from our national agencies: Fonds de la Recherche Scientifique-FNRS and Institut InterUniversitaire des Sciences Nucléaires for Belgium; MoSES for Croatia; CNRS and IN2P3 for France; BMBF for Germany; INFN for Italy; JSPS, MEXT, QFPU-Global COE programme of Nagoya University, and Promotion and Mutual Aid Corporation for Private Schools of Japan for Japan; SNF, the University of Bern and ETH Zurich for Switzerland; the Russian Foundation for Basic Research (Grant No. 12-02-12142 ofim), the Programs of the Presidium of the Russian Academy of Sciences (Neutrino physics and Experimental and theoretical researches of fundamental interactions), and the Ministry of Education and Science of the Russian Federation for Russia, the National Research Foundation of Korea Grant No. 2011-0029457 and TUBITAK for Korea, and the Scientific and Technological Research Council of Turkey for Turkey. We thank the IN2P3 Computing Centre (CC-IN2P3) for providing computing resources.

<sup>[1]</sup> K. Abe et al., Phys. Rev. Lett. 110, 181802 (2013).

<sup>[2]</sup> Y. Fukuda et al., Phys. Rev. Lett. 81, 1562 (1998).

<sup>[3]</sup> R. Bailey *et al.*, Report No. CERN-SL-99-034-DI, INFN-AE-99-05, 1999, addendum to Report No. CERN98-02, INFN-AE-98-05.

<sup>[4]</sup> R. Acquafredda et al., JINST 4, P04018 (2009).

<sup>[5]</sup> N. Agafonova et al., J. High Energy Phys. 11 (2013) 036.

<sup>[6]</sup> N. Agafonova et al., Phys. Lett. B 691, 138 (2010).

<sup>[7]</sup> A. Bertolin *et al.*, http://operaweb.lngs.infn.it/Opera/publicnotes/note161.pdf (2013).

<sup>[8]</sup> N. Agafonova *et al.*, New J. Phys. **14**, 013026 (2012).

<sup>[9]</sup> N. Agafonova et al., New J. Phys. 13, 053051 (2011).

<sup>[10]</sup> T. Fukuda, S. Fukunaga, H. Ishida, K. Kodama, T. Matsuo, S. Mikado, S. Ogawa, H. Shibuya, and J. Sudo, JINST 8, P01023 (2013).